10th International Symposium on Practical Design of Ships and Other Floating Structures
Houston, Texas, United States of America
© 2007 American Bureau of Shipping

The Impact of Fusion Welds on the Ultimate Strength of Aluminum Structures

Matthew D. Collette [1)]

[1)] Science Applications International Corporation
Bowie, Maryland, U.S.A.

Abstract

In the quest to minimize lightship weight, structural researchers and engineers are turning to limit-state design techniques for aluminum high-speed vessels (HSVs). In adapting techniques used for other materials for use on aluminum, one of the central problems faced is how to account for the reduced strength region in and around fusion welds in aluminum structures. The common marine aluminum alloys in both the 5000 and 6000 series alloys lose a significant portion of their strength when fusion welded. The properties of fusion welds in common marine alloys are reviewed in this paper, and previous work in this field is summarized along with new investigations into the tensile strength of such welds. Examples of loss of strength in tensile loading are given along with the implications for limit-state formulation and structural strength.

Keywords

Aluminum; Welds; Ultimate strength; Heat-affected zone (HAZ); Strain concentration.

Introduction

Aluminum high-speed vessels are being employed on increasingly demanding routes and missions by civilian and military operators around the world. As the roles of these vessels expand, there is growing interest in applying limit-state design techniques in the vessels' structural design and optimization in place of current allowable-stress techniques. Limit-state design has been extensively investigated for steel vessels, with many notable publications in this area. Paik and Thayamballi (2003) give an excellent overview of steel-based limit-state design. For steel structures, research to date has been dominated by limit states involving collapse following large deformations, fracture, and corrosion. Steel structures can usually be successfully idealized as having homogenous material properties within each member of the structure and usually only two or three grades of material are used within a single structure.

While the three failures modes – collapse, fracture, and corrosion – must be addressed with aluminum as well as steel, welded marine aluminum structures cannot normally be idealized as having homogenous material properties. Fusion welds in marine-grade aluminum are under-matched, or weaker, than the surrounding structure. Careful use of extrusions and friction-stir welding can significantly reduce the number of fusion welds in an aluminum vessel; however, at the present time it is not practical to remove all fusion welds from the structure. Transverse welds at frames and construction block boundaries are likely to remain for some time, along with longitudinal welds in places where extruded integral panels have not proven popular, such as bottom structure. In current allowable-stress design techniques, these under-matched welds can be accounted for by adjusting the allowable stress level in the structure, or treating the structure as if the entire structure was made of the weakest material, both of which impose a significant weight penalty on the structure. However, for limit state design where the non-linear collapse of the structure must be evaluated, this material inhomogeneity must be accounted for in the limit state formulations.

Fusion welds in marine alloys, such as the 5000 or 6000 series alloys, lead to a region of reduced strength near the weld, which is often referred to as the heat-affected zone (HAZ). For common marine alloys, the reduction in proof strength in this region is often on the order of 30%-50%, and the HAZ normally extends between 10mm and 30mm from the centerline of the weld. Thus, fusion welds are marked by pronounced material inhomogeneity in material strength, and this inhomogeneity occurs at a much smaller length scale than what characterizes the other dimensions of the structure, such as the panel length, which is normally on the order of 1 meter, and the vessel breadth and depth, which are on the order of 10 meters. This difference in length scales requires limit state models that are able to integrate both the local material failure near fusion welds and the overall structural failure modes that are similar to existing steel limit states. A similar situation can occur when high-strength steels are joined by under-matched welds, but the under-match in these joints is often closer to 10% than 50%.

One feature of the response of a structure with under-matched welds is that the plastic flow of the structure in the post-elastic regime is concentrated in the under-matched region. As this region is small compared to the overall dimensions of the structure, it is often possible to see ductile rupture in these regions when the average global strains of the overall structure are still quite low. This leads to an overall structural response and failure that can appear similar to a brittle failure, although it is important to note that the failure is still fundamentally a ductile failure on the local level. This limitation of ductility indicates that failure modes – such as rupture in tension – that are often not investigated for steel vessels may be important for aluminum vessels.

In the following sections, the implications of welds on the ultimate limit state of aluminum structures will be further explored. First a review of previous works in this field will be presented, followed by a detailed review of fusion welds in 5000 and 6000 series aluminum alloys. Simple models of a welded aluminum joint are reviewed, followed by a summary of existing data on the effect of welding in compressive collapse. The results of several new models and studies for the influence of welding on tension limit states are presented, and conclusions are drawn.

Review of Previous Work

As aluminum limit-state analysis is a relatively new area of research in the marine field, much of the existing work on aluminum welds originates from the civil engineering, offshore, and aerospace fields. However, similar issues have been tackled in the marine industry when examining under-matched welds used in conjunction with high-tensile strength steel, where using under-matched welds can reduce fabrication costs. Ship Structure Committee report SSC-384 (Dexter and Ferrell, 1995) presents a good overview of this work and several experimental investigations into shipbuilding steels. Additional significant aluminum studies are briefly reviewed below, presenting first studies on local weld behavior, followed by studies on in-plane compressive collapse of ship-like shell structures, in-plane tension and bending collapse, and lateral collapse.

Weld Properties

Several studies have experimentally investigated local material properties near aluminum fusion welds. Hill, Clark, and Brungraber (1966) present one of the first studies of the influence of welding on structural response. Scott and Gittos (1983) present tensile and toughness measurements for a range of 5083 and 6082 butt welds. Malin (1991) presents a detailed study of welds in 6061-T6 extrusions used for panels as part of temporary bridging. Övreas, Thaulow, and Hval (1992) present material properties and FEM analysis of 6000-series butt welds. Matusiak and Larsen (1998) present material properties near a 6082-T6 butt weld as well as deformation and strength studies on butt and fillet welds in 6082-T6. Hval *et al.* (1998) present similar data for numeric modeling of fracture in 6005 and 6082 alloys, while Missori and Sili (2000) present similar data.

Compressive Collapse

Several authors have investigated the impact of welds on the compressive collapse of shell structures, where the primary mode of failure is structural instability. Mofflin (1983) investigated a wide range of 5083 and 6082 alloy plates with welds on both the plate boundaries parallel to the applied load and in the mid-region of the plate perpendicular to the applied load. Additionally, three panel tests have incorporated either longitudinal or partial transverse welds (Clarke and Swan 1985, Zha and Moan 2001, and Aalberg *et al.* 2001). Kristensen (2001), Paik and Duran (2004), and Rigo *et al.* (2003) performed numerical modeling of plates and stiffened panels including welds in compression. These studies have indicated that both longitudinal and transverse welds will impact the structure's strength in compression. In general, it is easier to formulate methods that include the effects of longitudinal welds on the ultimate strength, but transverse welds in the panel's mid-region can have a large impact on the predicted strength, especially for structures with low slenderness.

Tensile Collapse

There have also been several investigations into tensile collapse of welded aluminum structures, investigations that tend to focus on the reduction of ductility in a structure with under-matched weld regions and the related influence either on impact or crash resistance or on plastic capacity. The majority of the work to date has focused on plastic capacity under quasi-static loading. In an aerospace application, Verderaime (1989, 1991) studied the response of a butt weld in 2219-T87 aluminum, including formulating a simple model to predict the response of the weld under tension and bending loading. A similar weld was investigated by Vaughan and Schonberg (1995). Hval, Johnsen, and Thaulow (1995) investigated the impact of welds on 6082-T6 frameworks for offshore applications, and estimated the reduction in ductility from such welds. Roberts and Newark (1997) investigated welds in 7000-series aluminum tapered plate girders, finding that the girders' shear capacity was limited by sudden fracture of the HAZ where the web meets the flange and panel breakers on the girder. Moen, Hopperstad, and Langseth (1999) investigated the rotational capacity of welded and unwelded 6082-T6 beams, noting that the failure mode of the welded beams was rupture in the tensile HAZ near the weld. More recently, Chan and Porter Goff (2000) examined welded finger connections in 7000-series alloys, and formulated a weld failure model considering the material properties in the HAZ. Wang, Hopperstad, Larsen, and Lademo (2006) formulated and tested a finite-element approach for modeling the fillet weld connection in aluminum alloys.

While the studies above focus primarily on quasi-static loading, the weak region near welds also causes concern for impact and crash loading. An extensive European

Union project, ALJOIN (2007), has investigated "unzipping" of fusion welds in 6000-series aluminum rail cars during accidents, where the welds fail with little deformation of the surrounding structure. Such failure modes may be relevant for ship structures under collision, grounding, or blast loading.

Collectively, these studies represent a large body of work examining the tensile response of aluminum welds. These studies indicate that the weaker region near the welds can significantly impact the overall strength and ductility of the structure, and that an understanding of the properties of the local region around the weld is important when moving towards a limit-state design approach.

Lateral Collapse

The impact of welds on the strength of aluminum panels loaded laterally, or out-of-plane, has not been investigated as extensively as in-plane loadings. Abildgaard, Hansen, and Simonsen (2001) investigated the lateral plane response of welded plates through both experimental means and the use of a yield-line theory approach. Again, the potential for fracture or premature failure in the HAZ was noted.

Properties of Welds in 5000 and 6000 Series Alloys

The response of welded aluminum depends strongly on the underlying metallurgy of the particular aluminum alloy. 5000 and 6000-series alloys are the two most commonly used alloys in marine construction, and the metallurgy and resulting material properties of each will be reviewed below. In this work, the Ramberg-Osgood stress-strain relation will be used to model the response of the aluminum alloy. While this relation may not always capture the profile of the entire stress-strain curve, it has the advantage of being simple and useful for both analysis and design activities, where the type of data required for more advanced models may not always be available. The Ramberg-Osgood relation relates applied stress, σ, to strain, ε, via the material's elastic modulus, E, a proof stress $\sigma_{0.2}$, and an exponent, n.

$$\varepsilon = \frac{\sigma}{E} + 0.002\left(\frac{\sigma}{\sigma_{0.2}}\right)^n \quad (1)$$

Sample parameter values for common alloys are show in Table 1.

Table 1: Typical material properties for thin 5000 and 6000 series marine alloys (Strengths are minimums per ABS 2006, Ramberg-Osgood exponents are typical)

Property	5083-H116	6061-T6
Un-welded proof stress	214 MPa	241 MPa
Un-welded ultimate stress	303 MPa	262 MPa
Un-welded RO exponent, n	12	29
Welded proof stress	165 MPa	138 MPa
Welded ultimate stress	276 MPa	165 MPa
Welded RO exponent, n	8	16
Approximate failure strain	8%	10%

5000-Series Alloys

The 5000-series alloy is one of the most common aluminum alloys used in marine construction; it is typically used for shell plating, although it is possible to extrude it. In the 5000-series, the primary alloying elements is Magnesium, and the resulting microstructure can be made stronger by cold-working or strain hardening the alloy. The marine tempers of –H116 or –H321 have had a significant amount of strain hardening. When fusion welded, the high heat of the welding process anneals the alloy and causes the metal to loose its strain hardening in the region around the weld. The resulting weld will show smooth decline in material properties, with a minimum strength typically located near the center of the weld. A typical hardness profile of a 5000-series weld is shown in Fig. 1. While the weld region has a noticeably lower proof stress than the surrounding metal, it retains the ability to strain-harden, and as such the reduction in ultimate stress of the weld region is typically much smaller than the reduction in proof stress. Sample material properties are given in Table 1 and the corresponding stress-strain curve is presented in Fig. 2

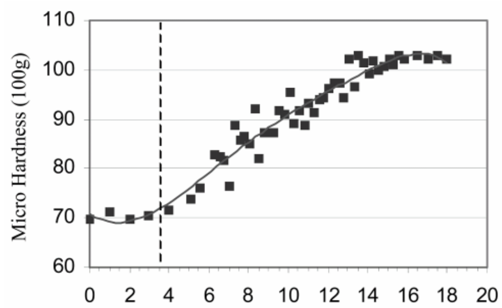

Fig. 1: 5000-Series Weld Hardness Profile (Paik and Duran, 2004)

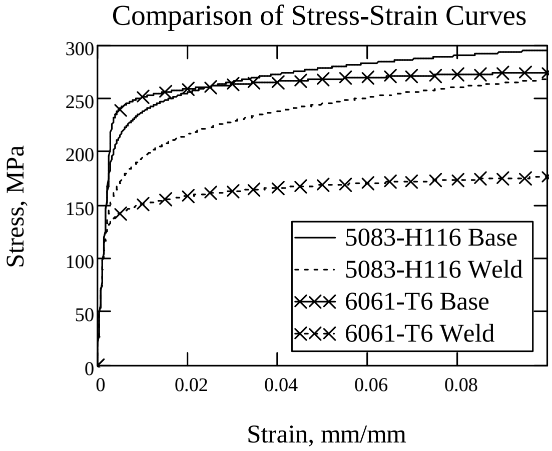

Fig. 2: Comparison of Stress-Strain Curves for Alloys

6000-Series Alloys

The 6000-series alloys commonly encountered in marine construction are in the form of extruded profiles or custom shapes. In this series, the primary alloying elements are Magnesium and Silicon, which are added so that Magnesium Silicide precipitates are formed by heat treating. Controlling the size and distribution of these precipitates allows tempers with high-strength to be developed. In a 6000-series fusion weld, the weld heat input will cause the weld metal and base metal immediately adjacent to the weld to reach a high enough temperature that the Magnesium Silicide will go back into solution and then re-precipitate over time, a process known as natural aging. Near the weld centerline, the weld may recover a significant portion of its pre-welded strength; however, at some distance off the centerline, the temperature will not be high enough to place the Magnesium Silicide back in solution and the precipitates will grow in size, a process known as over-ageing. This over-aged zone will be weaker than either the base material or the weld material, resulting in a "W" shape distribution of strength through the weld, as shown in Fig. 3 Depending on the choice of filler metal and weld process parameters, the central hump in the "W" may be more or less pronounced. Additionally, the 6000 series does not strain harden as readily as the 5000 series, so both the proof stress and ultimate stress of the material will be significantly impacted by welding; this impact can be seen in Table 1 and in the stress-strain curve plotted in Fig. 2.

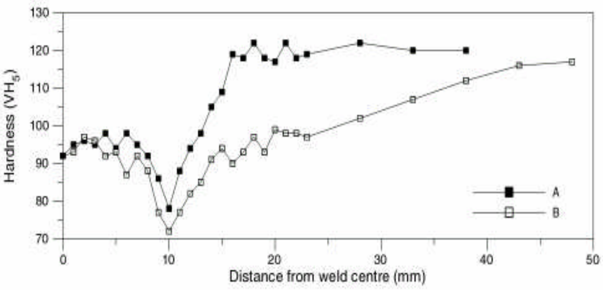

Fig. 3: 6000-Series Weld Showing "W" Hardness Profile at two locations, A, B, and over-aged zone 0.3-0.6" away from weld (Wang, Hopperstad, Larsen, and Lademo 2006)

Tension Weld Models

The previous work on aluminum structures has indicated that the tensile plastic capacity of welded aluminum structures may be less noticeable than the un-welded material properties, and the concentration of plastic strains in the weak regions around the weld may make the structure susceptible to failure at very low global strains. Thus, a logical place to begin a limit state analysis of welded structures is to investigate the tensile response of welds. There are several locations in typical aluminum vessel structures where welds will be subject to stress perpendicular to the direction of welding, including:

- module and building block joints
- fillet welds at the intersection of web frames and plating
- fillet welds joining sandwich-type deck extrusions to bulkheads.

Such connections in the strength deck or bottom structure may be subject to high levels of in-plane loading, and thus it is important to check for rupture potential in these welds when investigating global limit states of the hull girder. Additionally, it is important to determine the effective stress-strain response of the welded connection in tension in order to determine the total resistance force and moment for compressive collapse limit states elsewhere in the hull girder.

Series Model

The most basic model of a welded connection is a simple series model where the total strain across a series of *i* different "zones" in the weld is combined under the assumption that each zone acts independently of each other and that the total force, *F*, on each zone is equal according to

$$\varepsilon_{TOTAL} = \frac{\sum_i \varepsilon_i L_i}{L_{TOTAL}} \tag{2}$$

where ε is the strain, *L* is the length of each zone and the total length. While very simple, this model can provide useful insight for interpreting tensile test specimen results and understanding the relative importance of the different material parameters on the weld's capacity. Fig. 4 shows the results of applying such a model to a simple weld specimen with a 50mm HAZ. The HAZ was assumed uniform, and the material properties were as per Table 1, where a 10" gauge length is implied for proof stress measurements. Fig. 4 shows that, as the gauge length increases, the apparent proof stress of the specimen increases while the overall specimen strain at failure decreases, to less than 1% for the 6061 specimen. This is a result of inelastic strains building up in the HAZ once the applied stress exceeds the proof stress in the HAZ. The ductility of the specimen is then governed by the HAZ, and larger gauge lengths do not significantly increase the overall deformations because the added gauge material only undergoes comparatively low elastic strains. The ability of the 5000-series welds to strain harden in the HAZ means that the strain concentration is significantly less in 5000-series than it is in 6000-series alloys. This graph also clearly demonstrates that proof stress and gauge length are interrelated for inhomogeneous specimens.

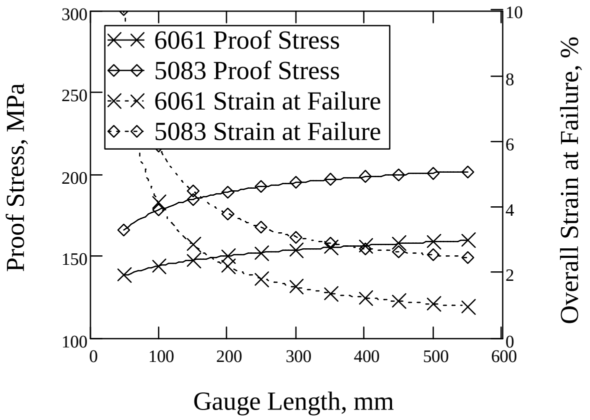

Fig. 4: Comparison of Proof Stress (Solid Lines) and Overall Strain at Failure (Dotted Lines) for Two-Zone Series model with 50mm HAZ

Three-Dimensional Model

There are several objections to applying the simple series model presented above to structures that are more complex than simple weld tensile specimens. In large welded structures such as aluminum HSVs, there are significant structural constraints working on most of the welds of interest: consider a transverse block join butt weld or the HAZ in front of a web frame fillet weld subjected to longitudinal stress. The neighboring base material that does not undergo large plastic strain with the HAZ will attempt to restrain HAZ contractions parallel to the weld and through the thickness of the material at the HAZ/base material interface; at the same time, volume conversation requires the HAZ material to shrink parallel to the weld and through the thickness of the plate as it elongates perpendicular to the weld. Several authors have proposed approaches that consider these effects. A model proposed by Satoh and Toyoda (1970) for a transverse weld in an infinitely wide plate is presented here. This model assumes that the weld can be modeled as a two-material combination, that the base metal can be assumed to be totally rigid compared to the weld metal, and that the weld will deform as a necked specimen as loading increased, as show in Fig. 5.

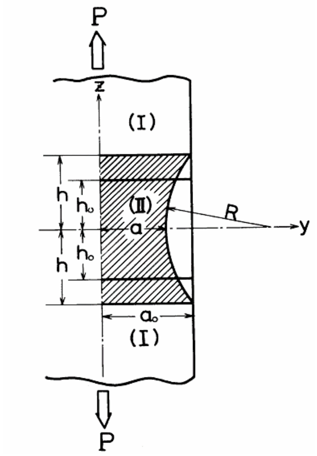

Fig. 5: Assumed weld deformation pattern by Satoh and Toyoda (1970)

In the model of Satoh and Toyoda, the stress-strain curve is represented by a simple power law, relating equivalent stress σ to strain ε by two coefficients K and n:

$$\overline{\sigma} = K\overline{\varepsilon}^{n} \tag{3}$$

It is assumed in the infinite weld that the true strain in the x-direction (along the length of the weld) is zero, and thus true stress, s, in the x-direction is equal to the average stress in the y and z directions. Thus the von Mises yield condition simplifies to:

$$s_Z - s_Y = \frac{2}{\sqrt{3}}\overline{\sigma} \tag{4}$$

By making some assumptions about how the stresses are distributed in the necking region of the weld, the equivalent stress can be related to the true strain perpendicular to the weld, e_z, through the relation

$$\overline{\sigma} = \left(\frac{2}{\sqrt{3}}\right)^{n} K e_z^{n} \tag{5}$$

and the engineering axial stress perpendicular to the weld, σ_z, can be related to the engineering strain perpendicular to the weld, ε_z, by the equation

$$\sigma_Z = \left(\frac{2}{\sqrt{3}}\right)^{n+1} \frac{K\left\{\ln\left(1+\varepsilon_Z\right)\right\}^{n}}{1+\varepsilon_Z}\left(1+Y_T\right) \tag{6}$$

where Y_t is found by solving the following equation with h_0 and a_0 defined in Fig. 5:

$$X_t = \frac{h_0}{y_0}, \varepsilon = \frac{1}{1+\varepsilon_z}$$
$$X_t = \frac{1}{\sqrt{3}}\sqrt{\left(1-\varepsilon\right)\left\{\frac{2\varepsilon}{Y_t} - 3\left(1-\varepsilon\right)\right\}}\left(\frac{2\varepsilon+1}{3} - \frac{\left(1-\varepsilon\right)^2 Y_t}{2\varepsilon}\right) \tag{7}$$

Comparison of the Models

The simple series model and the three-dimensional model of Satoh and Toyoda were compared to a series of butt weld tension tests published by Scott and Gittos (1983). These were axial tension tests on 5083 and 6083 13mm thick plates, joined by fusion welds. The 5083 plates were welded with 5556A filler metal, while the 6082 plates were welded with both 5556A and 4043A filler metal. The welded tension test specimens consisted of a reduced-width tension coupon, where the width at the weld was 25mm. Thus, this experimental program falls between assumptions of the series model and the infinite-width approach from Satoh and Toyoda. Average material properties for the base and weld metal specimens are listed below in Table 2. These values were determined from 6.4mm round tensile specimens consisting of either all-base or all weld-metal. While this gives material that is data compatible with the presented models, it is insufficient to determine any variation in material property across the weld in the HAZ zone, which may be significant for welds such as the 6082 weld, where a combination of naturally-aged and over-aged metal may be present.

Table 2: Average proof stress, $\sigma_{0.2}$ ultimate stress, σ_{ULT}, and elongation at failure, ε_f for Scott and Gittos samples

Material	$\sigma_{0.2}$ MPa	σ_{ULT} MPa	ε_f %
5083 Base	189.8	333.0	20.8
5083 Weld w/5556A	155.0	318.0	28.5
6082 Base	273.8	300.2	19.0
6082 Weld w/5556A	139.5	284.0	20.5
6082 Weld w/4043A	127.5	233.7	11.7

The results from the two weld models are summarized in Tables 3 and 4 below. In applying both models, a HAZ extent of 25mm was assumed on each side of the weld centerline. Additionally, Scott and Gittos present elongation over two gauge lengths of 50mm and 75mm.

Table 3: Comparison of Predicted Ultimate Strains, %, for Weld Specimens at different gauge lengths (GL) for the Series and 3-D (Satoh and Toyoda Models)

Base Material Weld Filler	5083 5556A	6082 5556A	6082 4043A
Exp. – 50mm GL	15.5	9.0	6.5
Series – 50mm GL	28.5	20.5	11.7
3-D – 50mm GL	28.0	19.4	10.6
Exp. – 75mm GL	13.5	7.0	5.0
Series – 75mm GL	23.8	14.4	7.9
3-D – 75mm GL	21.1	13.4	7.2

Table 4: Comparison of Predicted Ultimate Stress, MPa, for Weld Specimens

Material Weld Filler	5083 5556A	6082 5556A	6082 4043A
Experiment	308.5	232.5	222.0
Series Model	318.0	286.0	233.7
3-D Model	292.5	281.6	248.9

Tables 3 and 4 show that neither of the prediction methods is entirely successful, and both appear to have trouble for the 6082 weld with the 5556A filler metal. Both approaches also overestimate the ductility of the 6082 welds. This could be a result of the actual failure taking place in a narrow over-aged zone in the weld, thus making the HAZ width effectively smaller than what was assumed here.

Influence of Welds in Tension on Global Limit States

While the impact of welds on the local ultimate limit state of beams and panels has been clearly demonstrated in a number of experimental studies, the influence of welds on global limit states has received less attention. An initial investigation was made into how the response of aluminum welds may impact one of the principal global limit states, such as hull girder collapse under bending moments. A box girder was used to represent a large stiffened-panel structure, as shown in Fig 6, with the properties as listed in Tables 5 and 6, including reduced 5083-H116 properties for compressive loading. The box girder features 5000-series bottom and sides, and a 6000-series top flange. This material use is broadly representative of the use of aluminum on high-speed vessels, where shell plating in contact with seawater tends to be 5000-series alloys, while large decks are often assembled from 6000-series extrusions. The box girder was tested under hogging moments to create a tension load on the 6000-series material in the top flange. The girder’s response was determined by applying an incremental curvature Smith-type approach (Smith 1977). An approximate response of the plate-stiffener combinations in compression was obtained using the simplified approach discussed in Collette (2005).

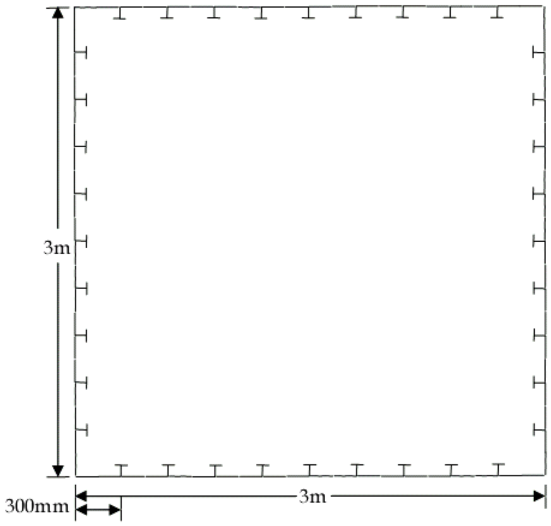

Fig. 6: Layout of box girder (not to scale)

Table 5: Box Girder Properties

Section	Plate mm	Stiffener Dimensions, mm	Matl.
Bottom	12	120x55x5.5x7.7 T	5083
Sides	8	80x45x4.5x6.2 T	5083
Top	6	70x40x4.0x6.1 T	6082

Table 6: Box Girder Material Properties

Property	5083-H116	6082-T6
Un-welded proof stress	180 MPa	260 MPa
Un-welded ultimate stress	305 MPa	290 MPa
Un-welded RO exponent, n	12	30
Welded proof stress	144 MPa	138 MPa
Welded ultimate stress	240 MPa	173 MPa
Welded RO exponent, n	8	16
Approximate failure strain	`12%	8%

The tension response of the top flange was modeled under three different assumptions:

- The tensile response of the material is represented by the base properties of the 6082-T6 alloy.
- The tensile response of the material is represented by all-weld properties of the 6082-T6 alloy.
- The tensile response of the material is represented by the application of the series-model presented in this paper. This model was adjusted to include the effects of longitudinal welds as well as transverse welds.

The three different responses of the top flange are shown in Fig. 7, and the corresponding response of the overall box girder in hogging is shown in Fig. 8. In Fig. 8, the response of a perfectly linearly elastic girder of the same cross section is also shown in heavy line for comparison. The results clearly indicate that the type of model assumed for the tensile response will have a noticeable impact on the computed ultimate strength of the girder. Notably, using the base material properties give unconservative predictions. Note that changing the effective resisting force from the tension flange also moves the neutral axis location, causing the peak in the moment-resisting curve to occur at different overall curvatures. The all-base material response has a sharper ultimate load, which occurs at an early curvature value than the cases where the impact of the HAZ is included. Such changes affect the strain levels that each component of the girder is subjected to during the loading. Another area of concern is the potential for fracture in the HAZ of the welds on the girder's tension flange, before the complete collapse of the compression flange, although results on two similar girders (Collette, 2005) indicated that the bottom structure must be quite stocky, and the fracture strain must be quite low in the HAZ for this to occur. For all of these reasons, it is important to have a solid local model for the response of welds when considering global failure modes for aluminum structures.

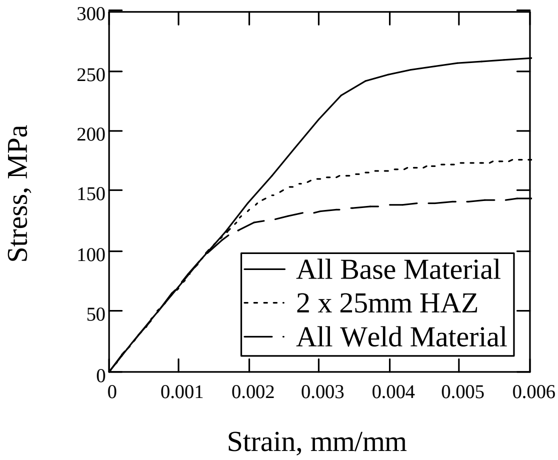

Fig. 7: Tensile Response of Deck Panels

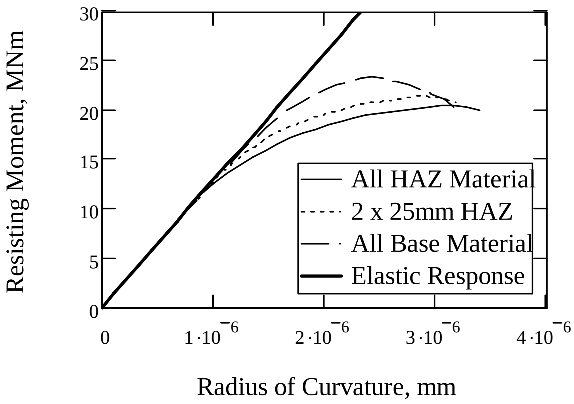

Fig. 8: Overall Resisting Moment Vs. Curvature, Hogging Loading

Conclusions

The impact of fusion welds on aluminum limit states was examined during the effort described in this paper. It is clear that the under-matched HAZ near welds in aluminum structures may accumulate plastic strains much faster than the rest of the structure, and have a significant impact on limit state calculations. Existing work on the role of welds in aluminum limit states has focused mainly on the compressive and tensile failure of welds and HAZ in local structures. The metallurgy of the 5000 and 6000 series alloys was reviewed, showing that the metallurgy of 6000-series fusion welds makes them more susceptible to plastic strain concentration. Simple weld models were compared to experimental test data for 5000 and 6000 series butt welds. Fair agreement with the simple models was shown; however, the restraint on the test welds fell between the idealized restraint in the two theories which could impact the comparison. A comparison of a global hogging collapse limit state was made by applying a Smith-type approach to a box girder, with three different tension weld models. The resisting moment plots are different in both magnitude and shape, indicating that the local tensile weld model may have a noticeable impact on global limit states. As the marine structural community moves towards limit state design for aluminum structures, it is clear that there is a need for practical limit-state models for aluminum welds.

Acknowledgements

The author wishes to thank Dr. Paul Hess of the Office of Naval Research (ONR) who has provided support for this work.

References

Aalberg, A., M. Langseth, and P.K. Larsen, (2001) "Stiffened Aluminium Panels Subjected to Axial Compression", Thin-Walled Structures, 2001. 39(10): 861-885.

Abildgaard, PM, Hansen, PW, Simonsen, BC, (2001), "Ultimate Strength of Welded Aluminium Strucutures", Proceeding of HIPER 2001, pp. 4-18.

ABS (2006), "Rules for Materials and Welding 2006: Part 2 Aluminum and Fiber Reinforced Plastics", Houston, TX: American Bureau of Shipping, 2006 including January 2007 update.

ALJOIN (2007), Project Website, http://www.aljoin.net/ accessed on April 30th, 2007.

Chan, TK, Porter Goff, RFD (2000), "Welded Aluminum Alloy Connections: Test Results and BS8118", Thin-Walled Structures, Vol. 36, pp 265-287.

Clarke, JD and Swan JW, "Interframe Buckling of Aluminium Alloy Stiffened Plating", Admiralty Research Establishment Dunfermline, 1985, AMTE(S) R85104. October, 1985.

Collette, M, (2005), "Strength and Reliability of Aluminium Stiffened Panels", PhD Thesis, School of Marine Science and Technology, University of Newcastle upon Tyne.

Dexter, R, and Ferrell, M (1995), "Optimum Weld-Metal Strength for High-Strength Steel Structures", Ship Structure Committee Report SSC-383, Washington DC, July 1995.

Hill, HN, Clark, JW, and Brungraber, RJ (1966). "Design of Welded Aluminum Structures", Journal of the Structural Division, Proceedings ASCE, Vol 86, No ST6, pp 101-124.

Hval, M, Johnsen, RH, Thaulow, C (1995), "Strength and Deformation Properties of Welded Aluminum Structures with Reference to Local Design and Material Properties", Proceedings of INALCO 1995 pp 167-182.

Hval, M, Thaulow, C., Lange, JH, Høydal, SH, and Zhang, ZL (1998), "Numerical Modeling of Ductile Fracture Behavior in Aluminum Weldments", Welding Journal Research Supplement, May, 1998, 208s-217s.

Kristensen, OHH., "Ultimate Capacity of Aluminium Plates Under Multiple Loads, Considering HAZ Properties", Department of Marine Structures, Norwegian University of Science and Technology, 2001.

Malin, V (1991). "Efficient Welding Fabrication of Extruded Aluminum Mat Panels", ElectroCOM GARD Report A1-161, September 1991. Available online via http://stinet.dtic.mil/ , Accession number ADA279638.

Matusiak, M, and Larsen, LK, (1998). "Strength and Ductility of Welded Connections in Aluminium Alloys", INALCO 1998, Cambridge, UK, April 1998, pp 299-310.

Missori, S, and Sili, A, (2000). "Mechanical Behaviour of 6082-T6 Aluminum Alloy Welds", Metallurgical Science and Technology, Vol 18, No 1, pp 12-18.

Moen, LA, Hopperstad, OS, Langseth, M (1999), "Rotational Capacity of Aluminum Beams Under Moment Gradient I: Experiments", Journal of Structural Engineering, Vol 125. No. 8 910-920.

Mofflin, DS, "Plate Buckling in Steel and Aluminium", Phd Thesis, University of Cambridge, 1983.

Övreas, L, Thaulow, C, and Hval, M (1992). "Effect of Geometry and Size on the Mechanical Properties of AlMiSi1 Weldments" INALCO 1992, Munich, Germany, Paper 10.1.

Paik, JK and Duran, A (2004),"Ultimate Strength of Aluminum Plates and Stiffened Panels for Marine Applications", Marine Technology, 2004, 41(3): 108-121.

Paik, JK and Thayamballi, AK (2003), "Ultimate Limit State Design of Steel-Plated Structures", Chichester, England: John Wiley and Sons, 2003.

Rigo, P, et al., "Sensitivity Analysis on Ultimate Strength of Aluminium Stiffened Panels", Marine Structures, 2003. 16(6): 437-468.

Roberts, TM, and Newark, ACB (1997). "Shear Strength of Tapered Aluminum Plate Girders", Thin-Walled Structures, Vol 29, No 1-4, pp 47-58.

Satoh, K and Toyoda, M (1970), "Static Strength of Welded Plates Including Soft Interlayer under Tension across a Weld Line", Transactions of the Japan Welding Society, Vol. 1 No. 2 pp 10-17.

Scott, MH, and Gittos, MF, (1983). "Tensile and Toughness Properties of Arc-Welded 5083 and 6082 Aluminum Alloys", Welding Journal Research Supplement, Vol. 62, Sept 1983, pp 243s-252s.

Smith, CS (1977), "Influence of Local Compressive Failure on Ultimate Longitudinal Strength of a Ship's Hull", Proceeding of PRADS 77, Tokyo, Japan, pp 73-79.

Vaughan, R, and Schonberg, WP, (1995), “An Inelastic Analysis of Welded Aluminum Joint”, Metallurgical and Materials Transactions B, Vol. 26B, pp 1253-1261.

Verderaime, V (1989), “Weld Stresses Beyond the Elastic Limit”, NASA Technical Paper 2935, available at http://ntrs.nasa.gov/search.jsp

Verderaime, V (1991), “Plate and Butt-Weld Stresses Beyond the Elastic Limit, Material and Structural Modeling”, NASA Technical Report 3075, available at http://ntrs.nasa.gov/search.jsp.

Wang, T, Hopperstad, OS, Larsen, PK, and Lademo OG, (2006), “Evaluation of A Finite Element Modeling Approach for Welded Aluminum Structures”, Computers and Structures, Vol. 84 pp 2016-2032.

Zha, Y and Moan, T, “Ultimate Strength of Stiffened Aluminum Panels with Predominantly Torsional Failure Modes”, Thin-Walled Structures, 2001. 39(8): 631-648.